Mechanism of energy transformations in shear magnetohydrodynamic flows

G. D. Chagelishvili
Abastumani Astrophysical Observatory, Avenue A. Kazbegi 2[a], 380060, Tbilisi, Georgia

T. S. Hristov
Space Research Institute, 6 Moskovska Street, 1000 Sofia, Bulgaria

R. G. Chanishvili and J. G. Lominadze
Abastumani Astrophysical Observatory, Avenue A. Kazbegi 2[a], 380060, Tbilisi, Georgia
(Received 2 March 1992)

Evolution of slow magnetoacoustic perturbations is used to demonstrate a new mechanism of plane Couette flow shear energy transformation. The initial uniform magnetic field is considered to be directed along the unperturbed flow velocity. We find that the amplification of waves is nonordinary—it occurs in a limited time interval and is anomalously strong. The unusual behavior is manifested also by the fact that the characteristic length scale of perturbation diminishes down to the dissipative scales not only due to nonlinear cascade processes, but due to a linear drift in the **k** space as well.

PACS number(s): 52.35.Bj

I. INTRODUCTION

As a rule, flows realized in Nature are sheared—i.e., the flow velocities have a shear in the direction perpendicular to the velocity. For example, flows in accretion disks, galaxies, and jets originated in some active galaxy nuclei (AGN); those in solar corona, etc., are sheared. This particularly explains the interest in the shear flows. Moreover, in shear flows the directed motion energy, due to the existence of shearing, may become transformed into other kinds of energy that diversify noticeably the phenomena picture. The growth of perturbations in shear flows has been investigated before. However, probably due to incomplete analysis of equations, the anomalously intensive transfer of shear flow energy to perturbations energy has not been found. The phenomenon in the absence of magnetic field is discussed in [1–3]. Herewith we demonstrate the novelty that this transfer leads to in the presence of magnetic field. In particular, here we show the possibility of slow magnetoacoustic wave amplification in infinite flows with constant velocity shear. The initial uniform magnetic field is directed along the flow velocity. The phenomenon we discuss here has quite a universal character—it is inherent for other types of plasma oscillations as well. Besides, the behavior of the perturbed quantities in time is not ordinary: at the beginning for certain wave-number values the usual slow magnetoacoustic waves (here we consider incompressible perturbations) with constant energy exist. This is followed by "switching on" of phenomena, which in the time scale, less than a wave period, effectively transform the shear flow energy into a slow magnetoacoustic wave. After this, the wave energy "is saturated" at a level which can exceed its initial value by several orders of magnitude. It is important that during the perturbation evolution the change of wave number occurs in the direction of the velocity shear (X), i.e., $k_x = k_x(t)$. The proposed amplification mechanism is effective for moderate values of the ratio $|k_x/k_y|$, where k_y is the wave number of the perturbation along the mean velocity of motion $\mathbf{U}_0(0, U_{0y}, 0)$. Since $k_x(t)$ changes linearly in time [Eq. (26)], it is clear that for large times the ratio $|k_x(t)/k_y|$ becomes large. Therefore the efficiency of wave amplification decreases and this leads to the saturation of its energy. Amplification of density waves in a shearing sheet has been thoroughly investigated in [4]. An essential difference between our model and the model from [4] is that in the latter the density waves encounter a barrier around the corotation radius and this barrier acts as a wave amplifier. All unstable modes in this case owe their origin ultimately to the corotation amplifier.

Section II presents the mathematical formalism and the basic equations are obtained. The results from the numerical solutions and the analysis of the processes are considered in the third section. Detailed discussion of the energy transformations is presented in the fourth section.

II. MATHEMATICAL FORMALISM

Let us consider incompressible, unlimited, ideal flow in the presence of magnetic field. It is described by the following system of equations:

$$\mathrm{div}\mathbf{U} = 0 , \tag{1}$$

$$\frac{\partial \mathbf{U}}{\partial t} + (\mathbf{U}\nabla)\mathbf{U} = -\frac{1}{\rho}\nabla p - \frac{1}{8\pi\rho}\nabla \mathbf{B}^2 + \frac{1}{4\pi\rho}(\mathbf{B}\nabla)\mathbf{B} , \tag{2}$$

$$\frac{\partial \mathbf{B}}{\partial t} = (\mathbf{B}\nabla)\mathbf{U} - (\mathbf{U}\nabla)\mathbf{B} , \tag{3}$$

$$\mathrm{div}\mathbf{B} = 0 , \tag{4}$$

where all designations are standard. Let us assume that the unperturbed flow velocity $\mathbf{U}_0$ is directed along the Y

axis and has linear shearing along the X axis

$$\mathbf{U}_0(0,U_{0y},0), \quad U_{0y}=Ax \ , \tag{5}$$

where A is the velocity shear parameter, which is considered positive. Further, it is clear that A^{-1} plays the role of a time scale. Let us assume also that the unperturbed magnetic field is homogeneous and is directed along the velocity of regular motion,

$$\mathbf{B}_0 \| U_0 \ . \tag{6}$$

Taking into account the incompressibility of the medium (ρ=const), splitting other quantities into regular and perturbed parts

$$p=p_0+p', \quad \mathbf{U}=\mathbf{U}_0+\mathbf{u}, \quad \mathbf{B}=\mathbf{B}_0+\mathbf{B}' \ , \tag{7}$$

from Eqs. (1)–(4) and taking into account (5) and (6), in linear approximation for perturbed quantities we get

$$\frac{\partial u_x}{\partial x}+\frac{\partial u_y}{\partial y}=0 \ , \tag{8}$$

$$\left[\frac{\partial}{\partial t}+Ax\frac{\partial}{\partial y}\right]u_x=-\frac{1}{\rho}\frac{\partial p'}{\partial x}-\frac{B_0}{4\pi\rho}\frac{\partial B_y'}{\partial x}+\frac{B_0}{4\pi\rho}\frac{\partial B_x'}{\partial y} \ , \tag{9}$$

$$\left[\frac{\partial}{\partial t}+Ax\frac{\partial}{\partial y}\right]u_y+Au_x=-\frac{1}{\rho}\frac{\partial p'}{\partial y} \ , \tag{10}$$

$$\left[\frac{\partial}{\partial t}+Ax\frac{\partial}{\partial y}\right]B_x'=B_0\frac{\partial u_x}{\partial y} \ , \tag{11}$$

$$\frac{\partial B_x'}{\partial x}+\frac{\partial B_y'}{\partial y}=0 \ , \tag{12}$$

i.e., we discuss two-dimensional perturbations and consider them to be homogeneous over the z coordinate. The set of equations (8)–(12) is homogeneous in time. But, as discussed in [5], the Fourier expansion of the perturbations over time in the shear flows leads to obstacles. Therefore we will try to solve the problem without Fourier expansion in time. For this purpose, let us introduce the system of coordinates with sheared axis X_1OY_1, with the origin and the Y_1 axis coinciding with those used in Eqs. (8)–(12) of the Cartesian system and X_1 moving with the unperturbed flow (see Fig. 1) [3,6]. It is equivalent to substitution of variables

$$x_1=x, \quad y_1=y-Axt, \quad t_1=t \ , \tag{13}$$

or

$$\frac{\partial}{\partial x}=\frac{\partial}{\partial x_1}-At_1\frac{\partial}{\partial y_1}, \quad \frac{\partial}{\partial y}=\frac{\partial}{\partial y_1} \ ,$$
$$\frac{\partial}{\partial t}=\frac{\partial}{\partial t_1}-Ax_1\frac{\partial}{\partial y_1} \ . \tag{14}$$

With the new variables, Eqs. (8)–(12) take the form

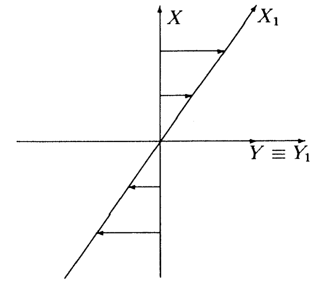

FIG. 1. Local Cartesian coordinate system XOY and the system with moving axes X_1OY_1 are presented. The arrows show the direction of the main flow velocity $\mathbf{V}_0$ at different distances from the Y axis. $\mathbf{V}_0(0,V_{0y},0)$, $V_{0y}=Ax$, $A>0$. The X_1 axis moves together with the shear flow.

$$\left[\frac{\partial}{\partial x_1}-At_1\frac{\partial}{\partial y_1}\right]u_x+\frac{\partial}{\partial y_1}u_y=0 \ , \tag{15}$$

$$\frac{\partial u_x}{\partial t_1}=-\frac{1}{\rho}\left[\frac{\partial}{\partial x_1}-At_1\frac{\partial}{\partial y_1}\right]p'+\frac{B_0}{4\pi\rho}\frac{\partial B_x'}{\partial y_1}$$
$$-\frac{B_0}{4\pi\rho}\left[\frac{\partial}{\partial x_1}-At_1\frac{\partial}{\partial y_1}\right]B_y' \ , \tag{16}$$

$$\frac{\partial u_y}{\partial t_1}+Au_x=-\frac{1}{\rho}\frac{\partial p'}{\partial y_1} \ , \tag{17}$$

$$\frac{\partial B_x'}{\partial t_1}=B_0\frac{\partial u_x}{\partial y_1} \ , \tag{18}$$

$$\left[\frac{\partial}{\partial x_1}-At_1\frac{\partial}{\partial y_1}\right]B_x'+\frac{\partial B_y'}{\partial y_1}=0 \ . \tag{19}$$

The transformation of the variables described in (13) is not a physical transition to the new frame, because in Eqs. (15)–(19) the quantities u_x, u_y, B_x', B_y' are components of the velocity and magnetic field perturbation in the Cartesian coordinate system. The coefficients of the initial linear equation system (8)–(12) depend on the space coordinate x. After our transformations, this inhomogeneity was changed into time inhomogeneity. So we can perform Fourier analysis of Eqs. (15)–(19) with respect to the variables x_1 and y_1:

$$\begin{Bmatrix} u_x \\ u_y \\ p' \\ B_x' \\ B_y' \end{Bmatrix}=\int dk_{1x}\,dk_{1y}\begin{Bmatrix} \tilde{u}_x(k_{1x},k_{1y},t_1) \\ \tilde{u}_y(k_{1x},k_{1y},t_1) \\ \tilde{p}(k_{1x},k_{1y},t_1) \\ \tilde{B}_x(k_{1x},k_{1y},t_1) \\ \tilde{B}_y(k_{1x},k_{1y},t_1) \end{Bmatrix}$$
$$\times\exp(ik_{1x}x_1+ik_{1y}y_1) \ . \tag{20}$$

Substituting expansion (20) into Eqs. (15)–(19) we obtain

$$(k_{1x}-k_{1y}At_1)\tilde{u}_x+k_{1y}\tilde{u}_y=0 \ , \tag{21}$$

$$\frac{\partial \tilde{u}_x}{\partial t_1} = -\frac{i}{\rho}(k_{1x} - k_{1y}At_1)\tilde{p} + ik_{1y}\frac{B_0}{2\pi\rho}\tilde{B}_x - i(k_{1x} - k_{1y}At_1)\frac{B_0}{2\pi\rho}\tilde{B}_y \ , \quad (22)$$

$$\frac{\partial \tilde{u}_y}{\partial t_1} + A\tilde{u}_x = -ik_{1y}\frac{\tilde{p}}{\rho} \ , \quad (23)$$

$$\frac{\partial \tilde{B}_x}{\partial t_1} = ik_{1y}B_0\tilde{u}_x \ , \quad (24)$$

$$(k_{1x} - k_{1y}At_1)\tilde{B}_x + k_{1y}\tilde{B}_y = 0 \ . \quad (25)$$

Using Eqs. (21)–(25) the evolution of the Fourier harmonic amplitudes represented by Eq. (20) may be traced. What does happen with these Fourier harmonics in the Cartesian coordinate system (XOY)? From (13), (14), and (20) the following relation may be obtained for the wave numbers in the direction X and Y at any time moment:

$$k_x(t) = k_{1x} - k_{1y}At_1, \quad k_y = k_{1y} \ ; \quad (26)$$

i.e., the wave number of each Fourier harmonic along the X axis changes in time. In other words, in the shear flow each Fourier harmonic drifts along the k_x direction.

This phenomenon may be traced by description of a Fourier harmonics package dynamics in the **k** space (Fig. 2). As it may be seen from Fig. 2 besides the package energy change, a drift in the **k** space takes place. As a result the energy density at a fixed point of the **k** space may increase from zero (at the initial moment) to some positive value (after certain time interval) (see point 1 in Fig. 2).

So, the usage of the variables x_1 and y_1 may be clarified. The description of a process using the Fourier harmonics which are obtained after an expression with respect to x_1 and y_1 coordinates resembles the description of a mechanical motion in Lagrangian coordinates (when the physical system is described by an observer moving together with it). In other words, Eqs. (21)–(25) describe the perturbation Fourier harmonics in the frame drifting with them in the wave-number space. In the $\mathbf{k}_1$ space this drift does not exist.

After simplifying Eqs. (21)–(25) and defining the dimensionless quantities

$$v_x \equiv \frac{\tilde{u}_x}{V_A}, \quad v_y \equiv \frac{\tilde{u}_y}{V_A} \ ,$$
$$b_x \equiv \frac{\tilde{B}_x}{B_0}, \quad b_y \equiv \frac{\tilde{B}_y}{B_0} \ ,$$
$$\omega \equiv \frac{V_A k_y}{A}, \quad \tau \equiv At_1 \quad (27)$$
$$k_x(\tau) \equiv k_{1x} - k_{1y}\tau \ ,$$

where $V_A = (B_0^2/4\pi\rho)^{1/2}$ is the Alfvén velocity, we get at last

$$\frac{\partial v_x}{\partial \tau} = \frac{2k_x(\tau)/k_y}{[k_x(\tau)/k_y]^2 + 1}v_x + \omega b_x \ , \quad (28)$$

$$\frac{\partial b_x}{\partial \tau} = -\omega v_x \ . \quad (29)$$

Our aim is to trace along the temporal evolution of the perturbation energy spectral density:

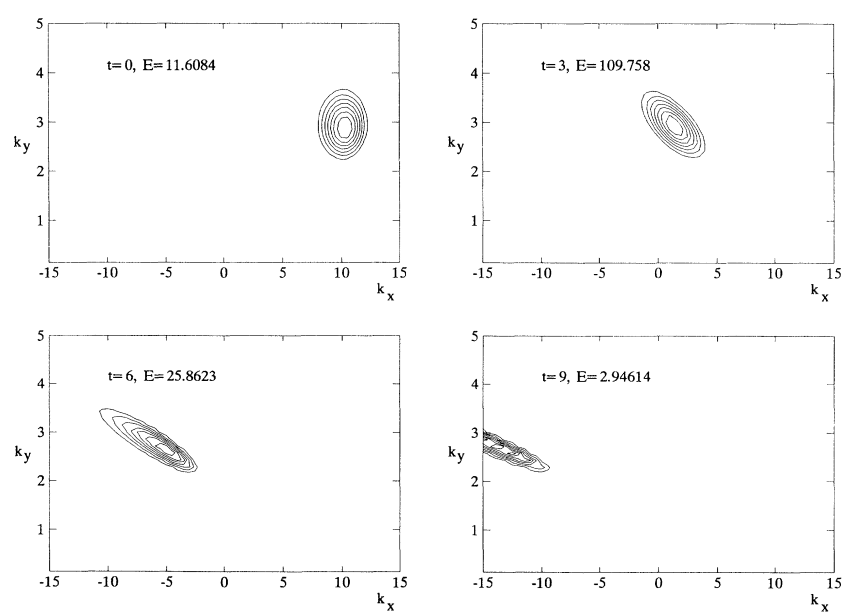

FIG. 2. Evolution of a package of perturbation Fourier harmonics is presented. The package accumulates energy in the region $k_x/k_y > 0$ and drifts in the wave-number plane. After a certain time interval the package is in the $k_x/k_y < 0$ region and there it completely returns its energy to the equilibrium flow.

$$W_{\mathrm{tot}}(k_{1x},k_{1y},\tau)=\frac{B_0^2}{8\pi}E_{\mathrm{tot}}$$
$$=\frac{B_0^2}{8\pi}(|v_x|^2+|v_y|^2+|b_x|^2+|b_y|^2)$$
$$=\frac{B_0^2}{8\pi}\left[\left[\frac{k_x(\tau)}{k_y}\right]^2+1\right](|v_x|^2+|b_x|^2)\ , \tag{30}$$

where $W_{\mathrm{tot}}(k_{1x},k_{1y},\tau)$ is the spectral density of the slow magnetoacoustic waves energy at the moment τ and in the point (k_{1x},k_{1y}) of the $\mathbf{k}_1$ space. But from above it is clear that $W_{\mathrm{tot}}(k_{1x},k_{1y},\tau)$ is the perturbation energy density at the moment τ in the point $(k_x(\tau),k_y)$ of the $\mathbf{k}$ space.

Using (21), (25), (28), (29), and (30) an equation for the evolution of W_{tot} (or E_{tot}) may be obtained:

$$\frac{\partial E_{\mathrm{tot}}}{\partial\tau}=2\frac{k_x(\tau)}{k_y}(|v_x|^2-|b_x|^2)$$
$$=2\frac{k_y}{k_x(\tau)}(|v_y|^2-|b_y|^2)\ . \tag{31}$$

It is clear that the Fourier harmonic energy increases for $k_x(\tau)/k_y>0$ and $|v_x|^2>|b_x|^2$ and for $k_x(\tau)/k_y<0$ and $|v_x|^2<|b_x|^2$. In other words, in the $k_x(\tau)/k_y>0$ case the shear flow energy is transferred to perturbation energy due to the perturbed motion of the media; in the $k_x(\tau)/k_y<0$ case the transfer is realized by the perturbed magnetic field.

III. NUMERICAL RESULTS AND DISCUSSION

Equations (28) and (29) without the first term on the right-hand side (rhs) in Eq. (28), describe ordinary slow magnetoacoustic oscillations with frequency ω in incompressible limit. It is known [7], that the slow magnetoacoustic waves do not affect the medium density when the Alfven velocity is much less than the sound velocity ($V_A \ll C_s$). Hence, all our calculations are related to the case of relatively weak magnetic fields. The first term of the right-hand side of Eq. (28) describes the energy transfer between the shear flow to the slow magnetoacoustic wave and therefore just this term brings qualitative novelty in the evolution of magnetoacoustic perturbations. The maximum value of the coefficient, multiplying v_x in the first term at the right-hand side in (28)

$$\alpha(\tau)=\frac{k_x(\tau)/k_y}{[k_x(\tau)/k_y]^2+1} \tag{32}$$

is reached when $\beta(\tau)\equiv k_x(\tau)/k_y=1$ and it is equal to 1. Therefore, the influence of this term is significant at $\omega<1$. The lower the frequency ω, the stronger the influence, and it is essential only in a limited time interval. For example, if at the initial moment of time $|k_x(0)/k_y|\gg1$, then $\alpha(0)\ll1$. Then if the value of ω is not too small, we have usual magnetoacoustic waves. According to Eqs. (26) and (32), $\alpha(\tau)$ increases in time and reaches its maximum value. Therefore, the influence of this term becomes important and if the value of ω is moderate, then the named influence is essential. For $\tau\to\infty$, $|k_x|\to+\infty$ so $\alpha\to0$ and again we get the usual magnetoacoustic waves. As it was shown by numerical solution, in the above-mentioned intermediate time interval, during which the deviation from the usual oscillation regime occurs, the energy of the wave increases anomalously. That is why from now on we will call it the amplification interval. Figures 3–8 represent the results of the numerical solution of the coupled equations (28) and (29). Figures 3 and 4 clearly show the amplitude growth of slow magnetoacoustic waves in the amplification interval for two values of the parameter ω: 0.1 and 0.01. In both cases $\beta(0)=100$. From these two figures it can be seen that the normalized spectral energy of wave E_{tot} in the amplification interval increases by several orders of magnitude, and the less the frequency ω, the bigger this increase (this conclusion is confirmed also by numerical simulations for other values of parameter ω, for example, $\omega=1$ and 0.001). The details of the wave evolution in the amplification interval are traced down on Figs. 5–8. From Fig. 7 it is seen that around the point $\tau=100$ (when the sign of $k_x(\tau)/k_y$ is changed) a considerable growth of b_x may be observed. On this fact the amplification of slow magnetoacoustic perturbations is based for the case $k_x(\tau)/k_y<0$.

The behavior of incompressible perturbations in free shear flows without magnetic field ($B_0=0$) has been investigated in [2,3]. There the analytical time dependence of v_x, v_y, and $v=(v_x^2+v_y^2)^{1/2}$ for $B_0=0$ is obtained:

$$v_x=v_x(0)\frac{[k_x(0)/k_y)]^2+1}{[k_x(\tau)/k_y]^2+1}\ , \tag{33}$$

$$v_y=v_y(0)\frac{[k_x(0)/k_y]^2+1}{[k_x(\tau)/k_y]^2+1}\left[1-\frac{k_y}{k_x(0)}\tau\right]\ , \tag{34}$$

$$v=v(0)\left[\frac{[k_x(0)/k_y]^2+1}{[k_x(\tau)/k_y]^2+1}\right]^{1/2}\ . \tag{35}$$

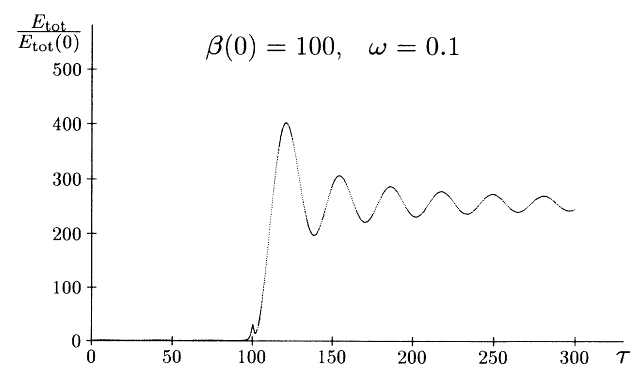

FIG. 3. Time dependence of $E_{\mathrm{tot}}/E_{\mathrm{tot}}(0)$ for $\beta(0)=100$, $\omega=0.1$, $v_x(0)=1$, $b_x(0)=0$. The graph shows the result of the numerical solution of Eqs. (28) and (29).

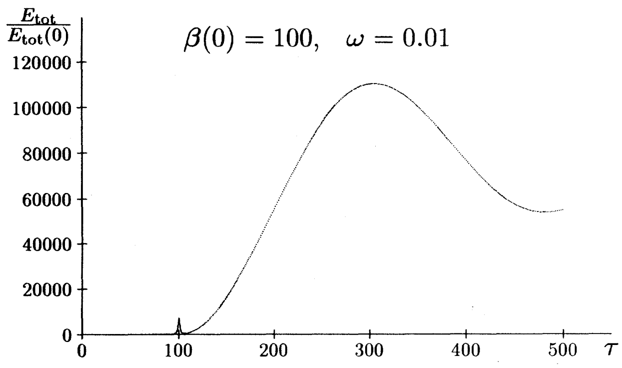

FIG. 4. Time dependence of $E_{tot}/E_{tot}(0)$ for $\beta(0)=100$, $\omega=0.01$, $v_x(0)=1$, $b_x(0)=0$. The graph shows the result of the numerical solution of Eqs. (28) and (29).

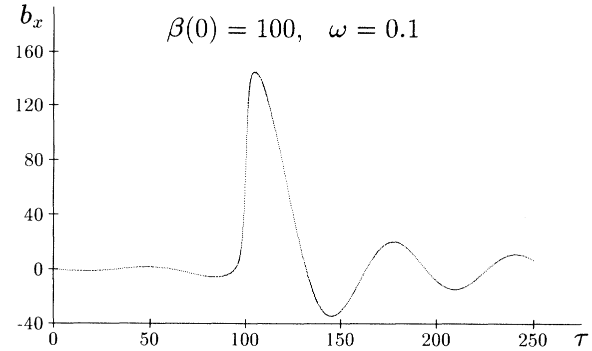

FIG. 7. Time dependence of b_x for $\beta(0)=100$, $\omega=0.1$, $v_x(0)=1$, $b_x(0)=0$.

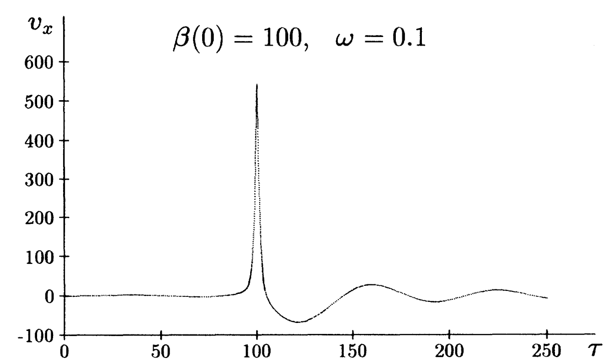

FIG. 5. v_x vs time for $\beta(0)=100$, $\omega=0.1$, $v_x(0)=1$, $b_x(0)=0$.

The results for $B_0=0$ are also plotted for comparison (see Figs. 9–11).

From the Figs. 9–11 and Eqs. (33) and (34) it is clear that in the absence of the magnetic field, for $k_x(\tau)/k_y>0$ (considering that $A>0$) the amplification of v_x occurs as well as that of the average energy of perturbations. Amplification happens at the expense of the unperturbed shear flow energy. In the course of time, when τ becomes more than $k_x(0)/k_y$ [i.e., $k_x(\tau)/k_y<0$], increase of the Fourier harmonic amplitude is replaced by weakening—perturbations return completely their energy to the equilibrium fields [for the case $b_x=0$ this is in agreement with (32)]. That is, if nonlinear phenomena do not switch on [1,2], perturbations disappear without leaving any traces. Amplification described just above is observed also in the presence of the magnetic field (small peak at time $\tau=100$ in Fig. 3). But unlike the case $B_0=0$, when $B_0\neq0$, as it is clear from Figs. 5–8, Fourier harmonics (in the frames of the linear theory approach) do not vanish without any traces. For $k_x/k_y<0$ the energy exchange between the shear flow and the perturbations due to the perturbed magnetic field switches on. As a result the perturbation energy is accumulated in the forms of oscillational kinetic energy (v_y) and magnetic energy (b_y). In the course of

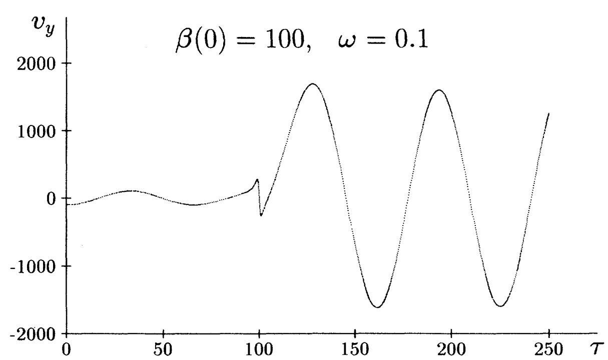

FIG. 6. v_y vs time for $\beta(0)=100$, $\omega=0.1$, $v_x(0)=1$, $b_x(0)=0$.

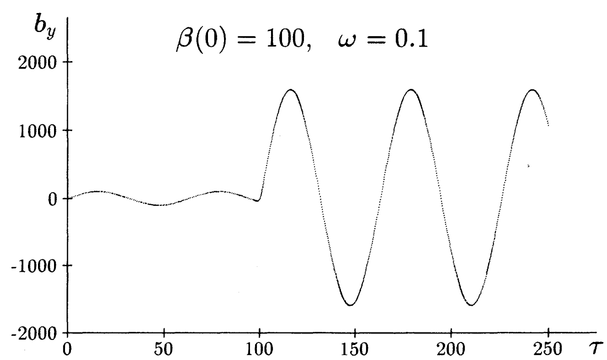

FIG. 8. Time dependence of b_y for $\beta(0)=100$, $\omega=0.1$ $v_x(0)=1$, $b_x(0)=0$.

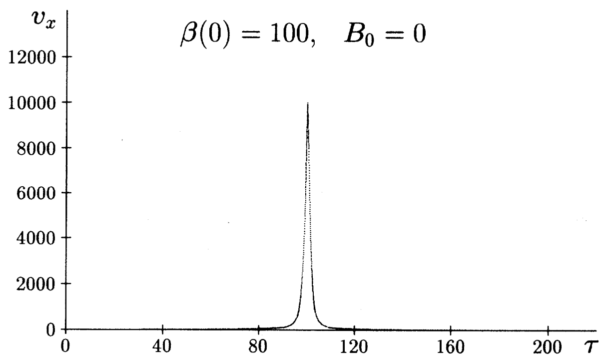

FIG. 9. Time dependence of v_x for $\beta(0)=100$, $B_0=0$, $v_x(0)=1$.

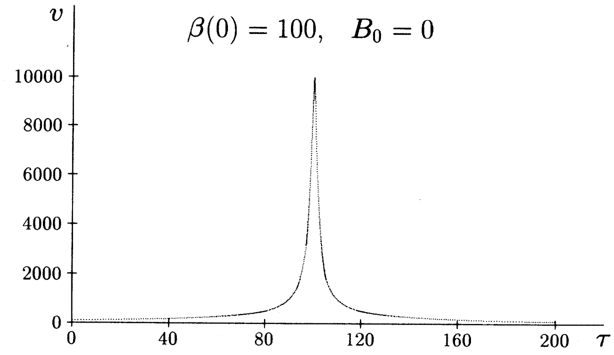

FIG. 11. Time dependence of $v=(v_x^2+v_y^2)^{1/2}$ for $\beta(0)=100$, $B_0=0$, $v_x(0)=1$.

time together with the increase of $|k_x/k_y|$, the amplifying action of the first term in the right-hand side of Eq. (28) approaches zero, so the oscillational action of the second term becomes dominant. But this occurs later for smaller ω. This circumstance may explain the fact that (as it was noted above) with the decrease of ω an increase of the accumulated energy of Fourier harmonics occurs. After this, as the second term at the right-hand side of Eq. (28) becomes predominant, the accumulation of energy stops and only magnetoacoustic oscillations with energy, considerably exceeding (depending on the value of $\omega \equiv k_y V_A/A$) the initial energy of the magnetoacoustic wave remains.

The level of the wave amplification also strongly depends on the phase with which the wave enters the amplification interval. The latter, in its turn, is determined by the phase of the wave φ_0 at the initial moment of time $t=0$. For slow magnetoacoustic waves the initial conditions can be assumed in the form $v_x(t=0)=\cos\varphi_0$ and $b_x(t=0)=-\sin\varphi_0$. (Figures 3–8 correspond to the $\varphi_0=0$ case). The dependence of the wave-energy growth on φ_0 for $\omega=0.1$ is presented in Fig. 12. The calculations show that for different values of φ_0 (i.e., different phases with which the wave enters the amplification interval) the rate of the energy growth of a slow magnetoacoustic wave for $\omega=0.1$ varies in the interval:

$$\frac{E_{\rm tot}(t\to\infty)}{E_{\rm tot}(t=0)}=1-900 \tag{36}$$

and for $\omega=0.01$

$$\frac{E_{\rm tot}(t\to\infty)}{E_{\rm tot}(t=0)}=8-10^5 . \tag{37}$$

The energy of the Fourier harmonic is accumulated in the components v_y and b_y (see Figs. 5–8).

IV. PHYSICS OF THE PROCESSES

To explain the energy transfer from the shear to the perturbations first we will describe the energy exchange between the shear flow and the perturbations in the $B_0=0$ case. We will consider Fourier harmonics, for which $k_x(0)/k_y>0$.

For that purpose let us examine a separate Fourier harmonic in the YOX plane and the planes of the fixed

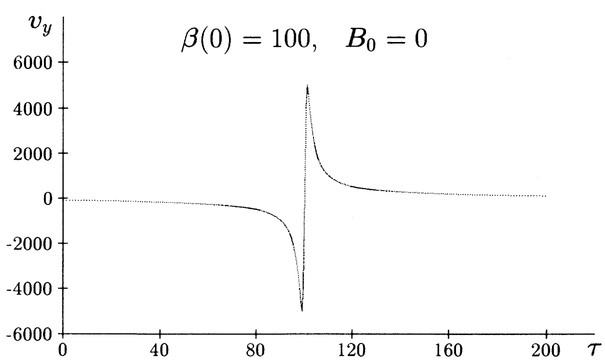

FIG. 10. Time dependence of v_y for $\beta(0)=100$, $B_0=0$, $v_x(0)=1$.

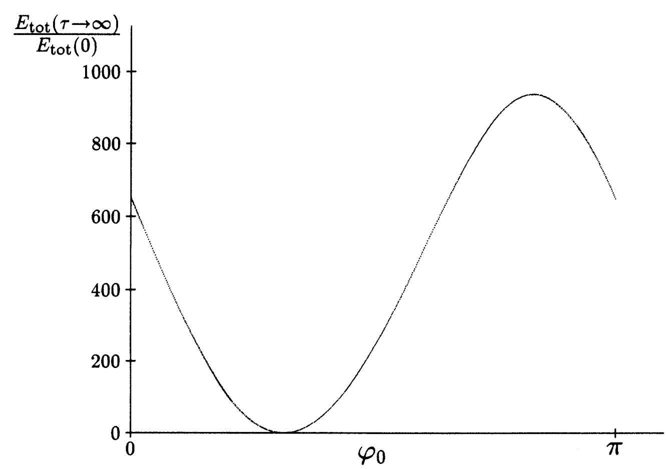

FIG. 12. Dependence of the amplification $E_{\rm tot}(\tau\to\infty)/E_{\rm tot}(0)$ on the initial phase φ_0 for $\beta(0)=100$, $\omega=0.1$.

phases at a given moment of time: $k_x(t)x+k_yy=2\pi m$ and $k_x(t)x+k_yy=\pi(2m+1)$, where $m=0,\pm1,\pm2,\ldots$ (see Fig. 13). Since we consider two-dimensional disturbances ($k_z=0$, $k_x,k_y\neq 0$), it is clear that the fixed phases planes are orthogonal to the plane YOX. As it follows from the incompressibility condition ($\mathbf{k}\cdot\mathbf{v}=0$) the vectors of the velocity perturbation are parallel to the fixed phases planes. Their directions, as well as those of the disturbance pressure forces can be seen from the same figure. The fixed phase planes shown in the figure are, at the same time, planes of the disturbance pressure maximums and minimums: The $-\nabla p$ forces are orthogonal to the planes. Accordingly, the planes of $p=\max$ can be conceived as walls elastically reflecting the fluid particles that run onto them. So, how is the shear flow energy converted into disturbance energy?

Let us single out a virtual element of the fluid (circle 1 in Fig. 13), located at a height x from the Y axis with the disturbance velocity $\tilde{\mathbf{v}}$. The unperturbed velocity of this element is $U_{0y}=Ax$. Because of the disturbance velocity $\tilde{\mathbf{v}}$ during some short time interval the chosen element drifts at the height at which the unperturbed flow velocity is given by the formula $U'_{0y}=A(x-\delta x)$. Thus the velocity of our element is greater than that of the unperturbed flow at the same height by $\delta U_{0y}=A\,\delta x$. So this is the velocity of its collision with the $p=\max$ wall. As a result of the elastic reflection from the wall, the total velocity of the element becomes

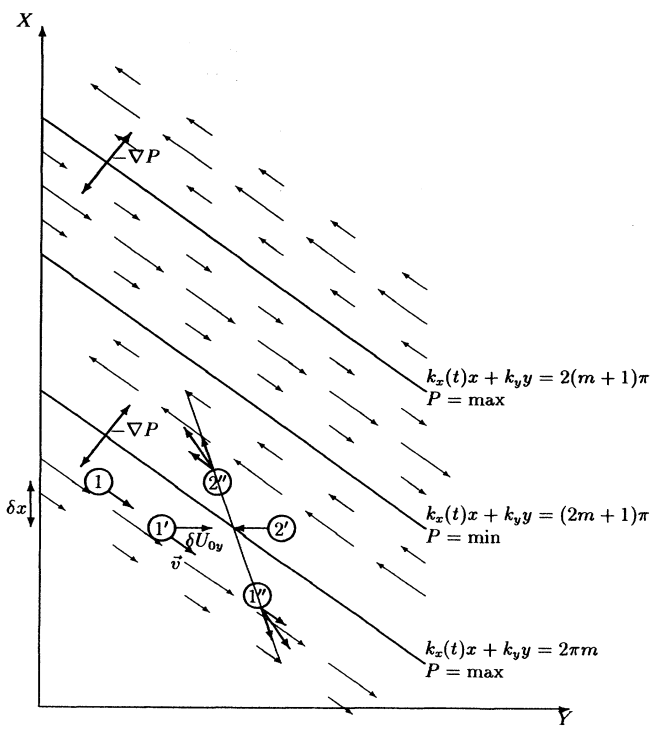

FIG. 13. Qualitative representation of energy transfer from the shear to the perturbations. The lines $k_x(t)x+k_yy=2\pi m$, $(2m+1)\pi$, $(2m+2)\pi$ represent the cross sections between the corresponding planes and the $Z=0$ plane. 1, 1′, and 1″ denote the same fluid element at different moments of time.

$$\mathbf{U}=\mathbf{U}'_{0y}+\tilde{\mathbf{v}}+\tilde{\mathbf{v}}' , \tag{38}$$

where $|\tilde{\mathbf{v}}'|=A\,\delta x$. That is, the disturbance velocity of the considered element becomes $\tilde{\mathbf{v}}+\tilde{\mathbf{v}}'$ (see Fig. 13). So, as a result of the processes just described the element's velocity changes by $\tilde{\mathbf{v}}'(\tilde{v}'_x,\tilde{v}'_y)$. In the case considered by us ($k_x/k_y>0$), the angle between $\mathbf{v}$ and $\mathbf{v}'$ is less than $\pi/2$. That is why $|\mathbf{v}+\mathbf{v}'|>|\mathbf{v}|$, i.e., the energy of the considered element increases due to its transfer from the main flow. This means that an amplification of the respective Fourier harmonic takes place. The variation of the disturbance velocity of the element 2 in the same figure may be described likewise.

The thorough consideration of the above scheme leads to the understanding that the elastically reflecting wall that we introduced into the picture acts, in fact, as an intermediary in the exchange of momenta between elements from the opposite sides of the wall for p at a maximum. For instance, we can treat the above case as an elastic collision of elements 1 and 2 shown in Fig. 13. It is clear from the above that the momentum exchange takes a place only when $\nabla p\neq 0$.

As can be seen from the process described above, the perturbation velocity of the considered element changes. This due to the incompressibility of the perturbations ($\mathbf{k}\cdot\mathbf{v}=0$) leading to change in the direction of the wave vector $\mathbf{k}$ of the considered Fourier harmonic. This is equivalent to a rotation of the fixed phases planes around an axis, perpendicular to the YOX plane. At the moment when the fixed phases planes of the Fourier harmonics become perpendicular to the Y axis the energy increase of the harmonic is interrupted. As the rotation continues, when $k_x/k_y<0$ the angle between $\mathbf{v}$ and $\mathbf{v}'$ becomes more than $\pi/2$. So, in the $|\mathbf{v}+\mathbf{v}'|<|\mathbf{v}|$ case the perturbation energy starts to decrease.

Let us now describe the physical mechanism of the energy transfer from the shear flow to the perturbation.

In the case which is investigated here, the energy transfer is realized not only by means of the perturbed motion of the medium but by means of the perturbed magnetic field as well. This process competes with those described above and instead of weakening [as in the $B_0=0$, $k_x(\tau)/k_y<0$ case] it leads to a considerable energy amplification of the slow magnetoacoustic perturbations (Figs. 3 and 4). But after, when the second term on the rhs of (28) becomes significant, the energy exchange between the shear flow and the perturbation is dominated alternatively by the perturbed motion and the perturbed magnetic field. In the $|k_x(\tau)/k_x|\gg 1$ case the first term on the rhs of (28) vanishes and a slow magnetoacoustic wave with constant energy propagates (see Figs. 3 and 4).

The degree of the perturbation spatial Fourier harmonic amplification obviously strongly depends on the length of the interval $[\tau_1,\tau_2]$ which in turn is determined by the normalized frequency ω. On the other hand, the amplification degree significantly depends on the position of $\tau=\tau_1$ over the time axis.

From Fig. 5 one sees that at the moment τ_1, v_x changes its sign (also unlike the $B_0=0$ case) and its value remains almost constant during a rather long time $\approx[\tau_1\tau_2]$. Although the value of v_x is small, in this case, v_y becomes rather large due to the increase of $|k_x(\tau)/k_y|$ (see Fig. 6). As seen from Figs. 7 and 8, b_y becomes large also. So, instead of decrease of Fourier harmonics energy, which occurs when $B_0=0$, in our case the character of the motion changes in such a way that the energy is accumulated in the forms of (v_y) and (b_y) of slow magnetoacoustic waves. The magnetic energy, mainly connected with the b_y component of the magnetic field perturbation, appears due to distortion of field lines of the unperturbed magnetic field by perturbed motion. The described accumulation of energy goes on until the oscillational action of the second term on the right-hand side of Eq. (28) becomes comparable (and dominant) with the amplificational action of the first term of the right-hand side of the same equation.

As shown here in free (unlimited) flows with constant shear ($U_{0y}=Ax$) the process of slow magnetoacoustic wave amplification occurs in an unusual way. The nonordinary results are obtained also due to the fact that the wave number along the shearing of the perturbations of the Fourier harmonics depends on time $[k_x(\tau)=k_{1x}-k_{1y}\tau]$. In particular in the course of time the characteristic length scale of an inhomogeneity along the X axis of the Fourier harmonics becomes smaller and smaller (for $\tau\rightarrow\infty$, $l_x=2\pi/|k_x|\rightarrow 0$). Usually the splitting of the perturbations length scale occurs due to the action of nonlinear (decay) processes [8,9]. But in our case the decrease of the length scale takes place in the linear theory as well. Hence, if after the amplification the level of slow magnetoacoustic waves becomes insufficiently high and nonlinear effects do not switch on, then the transition of perturbations energy to small length scales still will be ensured by linear processes. At small length scales the action of the dissipation effect becomes significant [8,9], so that ultimately all the energy of slow magnetoacoustic waves is transformed into heat. If we follow the main events, we may conclude that slow magnetic sound gains energy from the shear flow, accumulates it and transforms it to the small scales, converting it thus finally into heat due to the viscosity. This process can be described schematically in the k_yOk_x plane (see Fig. 14). We will consider here only the $k_y>0$ plane. This process can be reconstructed easily in the $k_y<0$ plane as well. Without taking into account the nonlinearity, the dynamics of magnetic sound, considered here, is governed by the following three processes: the Fourier harmonics drift in the $\mathbf{k}$ space, which is described by Eq. (26); the transfer of the shear flow energy to the perturbations, which is described by the first term on the right-hand side of the Eq. (28); viscous and Ohmic dissipation, which is not included in our equations, but the action of which can be easily understood. All these phenomena take place for any values of $\mathbf{k}$. But to clarify the discussion, the range of action of these phenomena in the $\mathbf{k}$ space can be differentiated. Let us assume that the viscous dissipation becomes essential for harmonics with wave numbers satisfying the inequality $|\mathbf{k}|>k_\nu$ (the region hatched by vertical lines outside the half circle in Fig. 14), where the value of k_ν depends on the viscosity. Let us assume also that the transfer of the shear flow energy to the energy of magnetic sound happens in the region dashed by the horizontal lines in Fig. 14 (the amplification region). On the level of thermal fluctuations in the medium there always exist perturbations of slow magnetic sound with arbitrary $\mathbf{k}$.

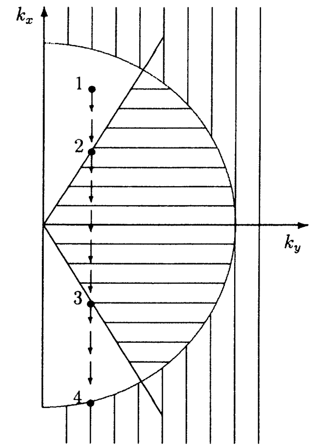

FIG. 14. Qualitative representation of the evolution of a slow magnetoacoustic perturbations in the k_xOk_y plane. In the horizontally hatched region the perturbations are amplified (Figs. 3 and 4). Outside, in the vertically hatched region, the perturbation energy is thermalized due to the viscosity and resistivity.

What is the way of the evolution of the Fourier harmonic which at the initial moment of time is at point 1 in Fig. 14? The wave number along the X axis of this harmonic changes in time and this leads to a drift in the direction marked by arrows. At some moment t when the harmonic appears at point 2, its anomalous energy growth starts and this lasts until it leaves the region of amplification (point 3 in Fig. 14). The level of increase in the region of amplification is defined by Eqs. (36) and (37). Then, the Fourier harmonic continuing its drift reaches point 4, where the dissipative processes switch on and convert the perturbation energy into heat. Other Fourier harmonics, which correspond to other points of the $\mathbf{k}$ plane evolve in a similar manner. After the Fourier harmonic leaves point 1, this point does not stay empty; due to the thermal effects new fluctuations appear which in turn evolve as described above. Thus, the transformation of the shear flow energy to perturbations together with the following dissipation is permanent and this naturally has to lead to a strong heating of the medium. It is clear that the heating intensity will depend on the level of the initial fluctuations and on the shear flow parameter A.

V. CONCLUSION

In the present paper, considering the slow magnetoacoustic perturbations in plasma, a new impressively strong mechanism of transformation of shear flow energy into perturbation energy and finally to heat is demonstrated. This may initiate a study of how the described mechanism acts for other waves in magnetoactive plasma. At the same time it must be taken into account that the incompressibility (div $\mathbf{v}=0$) of the perturbations is one of the necessary conditions for the effectiveness of the mechanism.

Finally we would like to note that the proposed mechanism of heating may be effective for AGN jets and solar corona, as long as the presence of the magnetic field there is doubtless. It may act efficiently also in some galactic and accretion disks, where toroidal magnetic fields, i.e., fields directed along the velocity of regular flow, also exist.

[1] G. D. Chagelishvili, R. G. Chanishvili, and J. G. Lominadze (unpublished).

[2] G. D. Chagelishvili, R. G. Chanishvili, T. S. Hristov, and J. G. Lominadze, in *Proceedings of the 23rd ESLAB Symposium on Two Topics in X-ray Astronomy, SP-296,* (ESTEC, Noordwijk, 1989).

[3] J. G. Lominadze, G. D. Chagelishvili, and R. G. Chanishvili, Pis'ma Astron Zh. **14**, 856 (1988) [Sov. Astron. Lett. **14**, 364 (1988)].

[4] R. Narayan, P. Goldreich, and J. Goodman, Mon. Not. R. Astron. Soc. **228**, (1987).

[5] K. M. Case, in *Hydrodynamic Instability,* edited by G. Birkhoff, K. Bellman, and C. Lin, in Proceedings of Simposia in Applied Mathematics, Vol. XIII (American Mathematical Society, Providence, 1962).

[6] P. Goldreich and D. Lynden-Bell, Mon. Not. R. Astron. Soc. **130**, 125 (1965).

[7] B. B. Kadomtsev (unpublished).

[8] L. D. Landau and E. M. Lifshitz, in *Fluid Mechanics,* Course of Theoretical Physics Vol. 6 (Pergamon, London, 1959).

[9] N. A. Krall and A. W. Trivelpiece, *Principles of Plasma Physics* (McGraw-Hill, New York, 1973).